Microsyst Technol (2008) 14:665–671
DOI 10.1007/s00542-007-0491-1

TECHNICAL PAPER

Three-dimensional simulation of sacrificial etching

Johann Cervenka · Hajdin Ceric · Siegfried Selberherr

Received: 1 June 2007 / Accepted: 5 November 2007 / Published online: 18 December 2007

Abstract Sacrificial etching is one of the most important process steps in micro-electro-mechanical systems technology, since it enables the generation of free-standing structures. These structures are often the main part of micro-mechanical devices, intended to sense or induce a mechanical movement. The etching process transforms an initial multi-segmented geometry and depends on material properties and several process conditions. One of the crucial issues for etching is the etching selectivity on different materials. The major task for the simulation is to give an answer, how sacrificial layer surfaces regress in time under the influence of process parameters and to which magnitude surrounding material segments are affected by the etching process. For this purpose we have developed a fully three-dimensional topography simulation tool, Etcher-Topo3D, which is capable to deal with realistic process conditions. The main concept is demonstrated in this work. During simulation the topography of the initial multi-segment geometry is changed which is handled by a level-set algorithm. After a simulation is finished, the level-set representation has usually to be converted back to a mesh representation to enable further analysis. To illustrate the main features of our simulation tool several examples of MEMS structures with a sacrificial layer are presented.

J. Cervenka (✉) · H. Ceric · S. Selberherr
Institute for Microelectronics, Technische Universität Wien,
Gusshausstrasse 27–29/E360, 1040 Vienna, Austria
e-mail: cervenka@iue.tuwien.ac.at

H. Ceric
e-mail: ceric@iue.tuwien.ac.at

S. Selberherr
e-mail: selberherr@iue.tuwien.ac.at

1 Introduction

Etching of sacrificial layers is a required process step in fabrication of micro-electro-mechanical systems (MEMS) devices. The use of a sacrificial layer is the key technique to release a micro-mechanical component from a substrate. In the process of sacrificial etching the sacrificial layer is selectively etched away leaving the structural layer which is part of the desired MEMS device capable of inducing or sensing a mechanical movement. Sacrificial etching most commonly utilizes polycrystalline silicon as the structural material and SiO_2 or phosphor–silicate–glass (PSG) (Liu et al. 1993) as the sacrificial material. Other combinations are for example: SiGe/SiO_2, Si_3N_4/polycrystalline silicon, and Si_3N_4/SiO_2 (PRIME Faraday Partnership 2002).

The subject of this work is wet sacrificial etching (PRIME Faraday Partnership 2002), e.g., to etch away PSG a water solution of hydrofluoric acid (HF) is applied. A typical etch rate with 2% HF at 20°C is about 0.8 μm/min. However, during sacrificial etching lower etch rates are observed because of additional effects like the transport of etch medium to the etch front and evacuation of the etch products (Mescheder 2004). In addition to HF etchants, also NH_4/HF solutions and HNO_3/HF acids are used to etch SiO_2. Another technological possibility is to use vapor hydrofluoric acid, which is referred to as dry etching (Bühler et al. 1997).

The control of the sacrificial etching process is carried out by several parameters such as the etch agent

concentration, temperature, and pressure. Besides these parameters, the formation of a sacrificial layer surface depends on local geometrical features and the nature of chemical reaction. In order to analyze these effects we have developed a three-dimensional topography simulation tool.

2 Modeling

The model for sacrificial etching consist of two parts. The first one has to describe the surface reaction with its moving boundary. The surface of the sacrificial layer represents an interface to the chemical solution in the reactor on which the chemical reaction takes place. In the case of etching sacrificial silicon dioxide layers by hydrofluoric acid, the chemical reaction on the surface of the sacrificial layer is (Liu et al. 1993)

$$6\mathrm{HF} + \mathrm{SiO_2} \longleftrightarrow \mathrm{H_2SiF_6} + 2\mathrm{H_2O}. \tag{1}$$

For the moving boundary problem a three-dimensional level-set algorithm is used (Sethian 1999). The level-set method describes surfaces and their evolution in time as the zero level-set of a certain function $\Phi(\mathbf{x}, t)$ (Heitzinger et al. 2002). The etch rate is interpreted as a speed function F of the level-set and calculated as

$$F = -\frac{\Delta\delta}{\Delta t} = -6J_{\mathrm{HF}}\frac{1}{\rho_{\mathrm{SiO_2}}}, \tag{2}$$

where $\Delta\delta$ is a small displacement of the etch front during time step Δt, J_{HF} is the flux of the etch agent on the sacrificial layer surface, and $\rho_{\mathrm{SiO_2}}$ is the mass density of silicon-dioxide.

Each surface point is moved with a certain speed. This leads to the level-set equation defined by

$$F|\nabla\Phi(\mathbf{x}, t)| = -\frac{\partial\Phi(\mathbf{x}, t)}{\partial t}, \tag{3}$$

where $\Phi(\mathbf{x}, t)$ represents the level-set function, delivering the evolving boundary, i.e., the etch front at $\Phi(\mathbf{x}, t) = 0$. Additionally, an initial condition $\Phi|_{\mathbf{x},t=0} = 0$, defining the initial etcher/material interface has to be defined. In this case $\Phi|_{\mathbf{x},t=0} = 0$ represents the entire surface of the initial geometry, which is exposed to the etch agent.

3 Selectivity

Due to the fact that etching processes in industrial reactors often include several segments of different material compositions, which are etched with different etch rates, the etching selectivity feature of the simulator enables prediction of an impact of unwanted material removal during etching of sacrificial segments.

The dependence of the materials on the etch rate is defined by a variable speed function defined on each interface point

$$F(\mathbf{x}) = F_{\mathrm{material}}(\mathbf{x}) \quad \text{for } \{\mathbf{x}|\Phi(\mathbf{x}, t) = 0\}. \tag{4}$$

4 Etch agent transport

The second part of the model describes the etch agent transport (Eaton and Smith 1996). This behavior is modeled with a second order partial differential equation

$$D\Delta c(\mathbf{x}, t) - \mathbf{u}\,\nabla c(\mathbf{x}, t) = \frac{\partial c(\mathbf{x}, t)}{\partial t}, \tag{5}$$

where c denotes the concentration of the etch agent, D is the diffusion coefficient, and $\mathbf{u}$ is referred as the back-flow velocity. The convective term $\mathbf{u}\,\nabla c(\mathbf{x},t)$ in (4) can usually be neglected compared to the diffusive term $D\,\Delta c(\mathbf{x},t)$ (Liu et al. 1993). If it is assumed that the system reacts in a quasi-static way, which means that the influence of transient processes $\partial/\partial t$ can be neglected, the resulting equation is the Laplace equation

$$D\Delta c(\mathbf{x}, t) = 0 \quad \text{for } \mathbf{x} \text{ inside the etchant domain.} \tag{6}$$

Since there is no need to perform a transient simulation of the transport, including a relatively complex discretization of the movement of the etch front, the solution can be calculated independently for each time step.

In order to fully determine the mathematical problem, the boundaries of the simulation domain have to be defined. We distinguish between three kinds of boundaries:

- The top of the domain, where the etch agent is delivered, which is modeled by constant concentration c_0 (Dirichlet boundary condition).
- The reactor walls. On these side-walls the etch medium cannot flow out. Usually the reactor is much bigger than the simulated domain, but also on the side-walls of the simulation domain conditions have to be defined. However, on these walls a vanishing out-flux of the medium is defined (Neumann boundary condition).
- The etcher/material interface. Here the etchant attacks the material, where different materials are usually etched with different etch rates. According to the reaction equation, the etchant is consumed, which is defined by an out-flux of etcher material through this boundary. This out-flux depends on the etcher concentration itself and on the involved materials

$$\begin{aligned}\frac{\partial c(\mathbf{x}, t)}{\partial \mathbf{n}} &= \nabla c(\mathbf{x}, t)\cdot\mathbf{n} = \nabla c(\mathbf{x}, t)\cdot\frac{\nabla\Phi(\mathbf{x}, t)}{|\nabla\Phi(\mathbf{x}, t)|}\\ &= J_{\mathrm{HF}} = f(\mathbf{x}, t, c(\mathbf{x}, t)) \qquad \text{for } \{\mathbf{x} \mid \Phi(\mathbf{x}, t) = 0\}.\end{aligned} \tag{7}$$

Various empirical forms of $f(\mathbf{x},t,c(\mathbf{x},t))$ can be found in (Eaton and Smith 1996) and have been examined by (Liu et al. 1993; Monk et al. 1993).

The relation between concentration and etch speed (Eqs. 2 and 6) couples both differential systems.

5 Discretization

The approximation of the level-set Eq. (3) is usually performed on an ortho-grid. For the discretization a second order upwind scheme based on finite differences is used. A common technique can be found in (Sethian and Adalsteinsson 1997).

However, the discretization of the second differential equation (6) is not limited to an ortho-grid. Usually a mesh is used which resolves the material boundaries properly. In order to prevent frequent remeshing of the domain, which is necessary because of the moving etch front, also an ortho-grid base with a special discretization which has the possibility to deal with the interface located between the grid points, is used.

Because of the simple coupling of the two systems and the quasi-static treatment a sequential calculation of Eqs. (3) and (6) is performed. First, a solution of the diffusion equation is calculated. Afterwards, the level-set equation is computed and the etch front is moved forward, as determined by the etch speed F. When consecutively applying these two steps until the final simulation time is reached, the final etch front given by the level-set function $\Phi(\mathbf{x}, t_{\text{end}}) = 0$ is determined.

For discretization of the diffusion equation the entire domain can be divided into four different regions:

1. The region resulting from the domain of etchant sources G_{S}. The etchant source is assumed to be at the top of the simulation domain at the grid points $p_s \in G_{\text{S}}$. The discretization simply reads

$$c_s = c_0 \quad \text{for } p_s \in G_{\text{S}}. \tag{8}$$

2. The etchant region G_{E}. For each grid point p_e of this domain, a simple finite boxes scheme is used, where each connection between points p_e and p_j delivers an additive contribution to its assigned equation. In summary, the equation can be written as

$$\sum_{\forall\, j,\, \exists\, \text{edge}<\text{p}_\text{e}\text{p}_\text{j}>} (c_j - c_e)\frac{A_{ej}}{d_{ej}} = 0 \quad \text{for } p_e \in G_{\text{E}}. \tag{9}$$

The parameters A_{ej} and d_{ej} denote the partial area of the Voronoi box between p_e and p_j and their distance, respectively. It should be noted, that also concentrations c_j of grid points p_j outside the etchant domain G_{E} are concerned.

3. The interface region G_{I}, which holds all grid points p_i connected to etchant points of G_{E}. These points hold a (virtual) concentration to account for the out-flux over the etch front. This virtual concentration is only necessary for discretization purposes. The resulting equations are built up by additive contributions of each connection connection p_e–p_i intersecting the etch front at p_{ei}, with

$$\sum_{\substack{\forall\, e,\\ \exists\, \text{edge}(\text{p}_\text{e}\text{p}_\text{i}),\\ p_e \in G_{\text{E}}}} \nabla c_{ei} \frac{\nabla \Phi_{ei}}{|\Phi_{ei}|} A_{ej} = \sum_{\substack{\forall\, e,\\ \exists\, \text{edge}(\text{p}_\text{e}\text{p}_\text{i}),\\ p_e \in G_{\text{E}}}} f_{ej} A_{ej} \quad \text{for } p_i \in G_{\text{I}}. \tag{10}$$

∇c_{ei} represents the discretized gradient in the intersecting point p_{ei}, $\nabla \Phi_{ei}$ is the discretized gradient of the level-set function. The out-flux at the etch front is determined by f_{ei}. Finally, A_{ej} is the according coupling area. A detailed two-dimensional view of an interface is shown in Fig. 1.

4. The remaining inside material region G_{M}. For reasons of a simple assembly of the equation system, the inside material region G_{M} (without the interface region) can be accounted for by equations with vanishing concentration

$$c_m = 0 \qquad \text{for } p_m \in G_{\text{M}}. \tag{11}$$

With this set of equations a system is built which has to be solved after each level-set extraction in order to deliver the new etchant concentrations. The equation system is of the general form

$$\mathbf{A} \cdot \mathbf{c} = \mathbf{f}. \tag{12}$$

The entries of $\mathbf{f}$ are not necessarily independent of $\mathbf{c}$, they depend on the chosen out-flux function $f = f(c)$. If f includes non-linear terms in c, a Newton scheme for solving the equation system has to be used. In cases of a

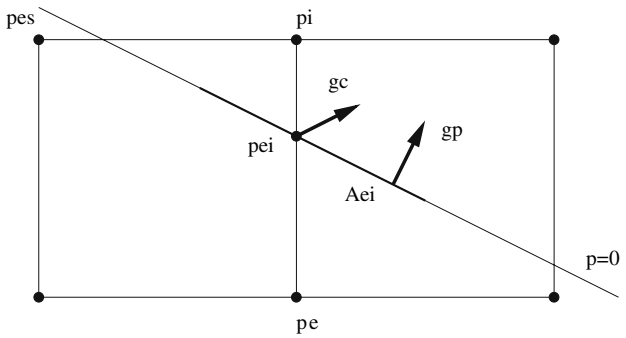

Fig. 1 Two-dimensional discretization of the etcher/material interface. The level-set $\Phi = 0$ intersects at p_{ei} between the grid points p_e inside the etcher atmosphere and p_i inside the solid. Characteristic parameters of the discretization are the gradient of the etcher front $\nabla\Phi$, the gradient of the etchant concentration distribution ∇c, and the assigned interface area A_{ei}

Fig. 2 Comparison of the etch front after a simulation with neglection and inclusion of diffusive transport

linear dependence, the linear terms in c can be moved to the left-hand side and the equation system can be solved directly.

A two-dimensional cut through a structure is shown in Fig. 2. This figure compares the etch front of a simulation with and without the inclusion of the diffusive transport. In the lower picture the governing out-flux function $f(c) = k\ c$ is used. The coloring of the etcher domain indicates the etchant concentration.

5.1 Determination of the Grid Spacing

In every discretization an error exists, which depends on the density of the mesh. Several aspects have to be considered to obtain an accurate result. First, the smallest desired geometry structures have to be resolved. Second, the distance function at a grid point represents the distance to its nearest interface. Accordingly, an error near geometry corners is produced. The selected grid spacing must be sufficiently small that these corner effects can be neglected. And finally, the diffusion dependent concentrations have to be resolved. The etcher/material interface is located somewhere between two grid points, one inside the etcher domain, one inside the material domain. The out-flux via the interface affects the concentrations of these points. For decoupling of the influence of different boundaries on a grid point, at least two grid points should be placed inside the smallest material layers. Therefore, an overall grid density two to three times higher than the smallest material layer thickness is used.

The discretization in time must use time steps smaller than the minimum grid spacing divided by the maximum speed (cf. Sethian and Adalsteinsson 1997) i.e.,

$$t_{\text{timestep}} < \frac{d_{\min}}{F_{\max}} \tag{13}$$

must be satisfied.

6 Combination with other Tools

Our simulation tool is also intended to work in combination with process simulation tools which are based on the finite element method. The original level-set ortho-grid used to solve the level-set equation holds also the representation of the new sacrificial material surface. The geometries defined by this new surfaces must be mapped to the geometries meshed by an unstructured tetrahedral mesh adequate for the finite element method.

The initial geometry is defined on a tetrahedral grid. Via sampling on the ortho-grid, the representation suitable for the level-set algorithm is achieved. After etching the etch front has to be converted back to a volume mesh. As the usually relatively simple input mesh cannot resolve the etch front properly, the initial mesh has to be refined. In our implementation the input tetrahedrons are split along their edges into smaller tetrahedrons. To reduce the overall size of tetrahedrons, a global refinement is not feasible (Wessner et al. 2003). The tetrahedrons are only split in regions, where the etch front passes through. But, only cutting along the etch front is also not suitable, because the quality of the tetrahedrons gets worse. As described in Rivara and Inostroza (1995) cutting of the longest edge preserves the quality. However, it is not guaranteed that this refinement procedure stays local in three dimensions. Our implemented algorithm is not as strict and delivers in practice good results.

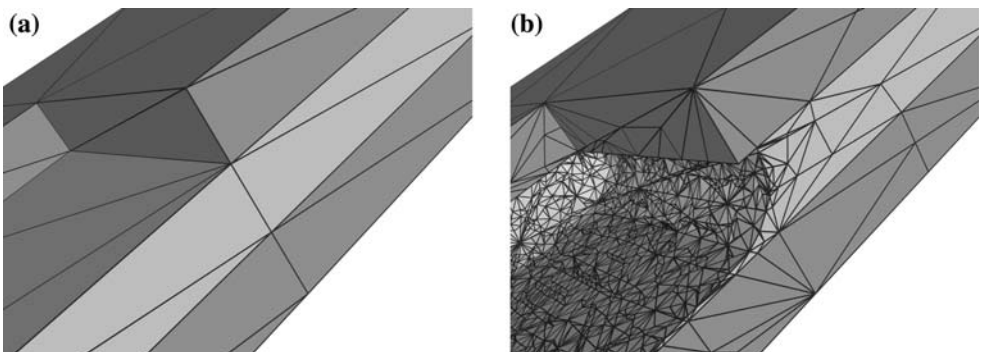

Fig. 3 Detail of a structure. *Left* the initial geometry with a crude mesh. *Right* after etching a tetrahedral mesh is reconstructed

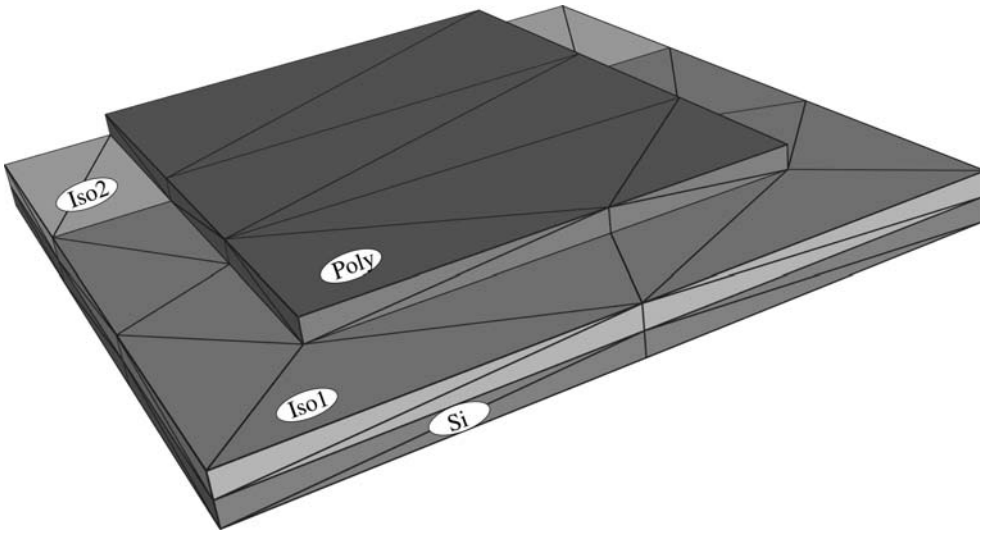

Fig. 4 Original material constellation on a tetrahedral mesh. The materials Iso1 and Iso2 are etched away

The algorithm works as follows: tetrahedrons are either split (until a minimum size is reached), if the etch front passes through or if a surrounding tetrahedron has been split and the resulting one has a too bad shape. Usually, an edge is split in the middle, resulting in very small tetrahedrons to resolve the front properly. In our implementation the tetrahedron is split on a suitable multiple as the etch front fraction. Afterwards, subsequent splits have only to be performed in the middle, which guarantees that the etch front is reached soon and without destroying the quality. Surrounding tetrahedrons are only split, if their longest edge differs from the actual one by a constant factor, thus lowering the tetrahedron quality only up to a tunable value. The detail of an etched structure, in comparison to the original structure, can be seen in Fig. 3.

7 Simulation results

In the following two typical examples are shown. The first one shows the evolution of the etch front of a sacrificial layer consisting of two materials with different etch rates. In the second example the etching of a cantilever structure with materials with highly different etch rates is shown.

7.1 Evolution of the Etch Front

Figure 4 depicts the initial constellation. A silicon wafer is coated by two isolation layers (Iso1 and Iso2) and on top of these layers, the actual polysilicon layer is deposited. Exposed to the etch agent the two isolation layers are etched away. Due to the fact that these two layers are of different materials, the etch rates are different, too. To demonstrate the selectivity feature of the etching model, material Iso1 is etched twice as fast as Iso2, all other materials are not attacked by the etch agent.

First, etching takes place at the planar surface down to the silicon layer, with a slight under-etch of the polysilicon layer (cf. Fig. 5). Due to the small isolation layer thickness this process finishes relatively fast. Now the free surface of the isolation is exposed to the etch agent and the etching front moves forward under the polysilicon layer, naturally, with different etch rates. The etch front after one minute is shown in Fig. 6.

Due to the nature of the applied level-set algorithm, the etch surface is represented on an ortho-grid. More detailed,

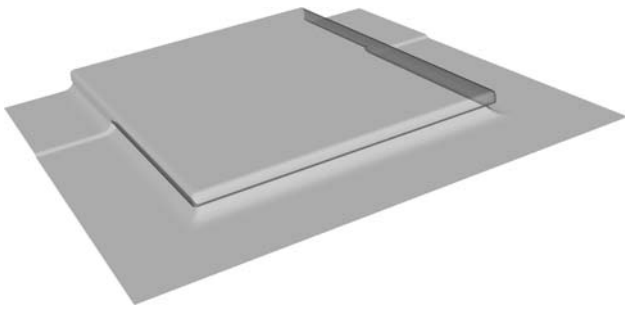

Fig. 5 The etching process started. First the former planar surfaces on top of the isolators are etched away

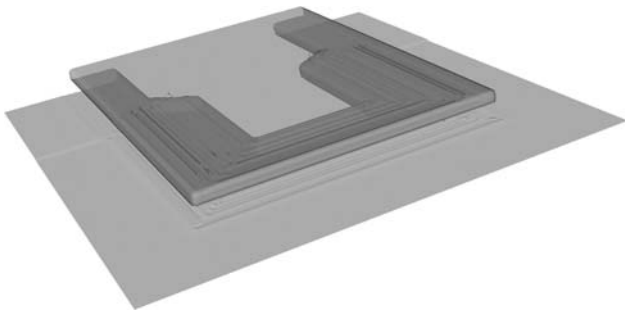

Fig. 6 During the etching process, the isolators are attacked. Material Iso1 has nearly twice the etch speed than Iso2

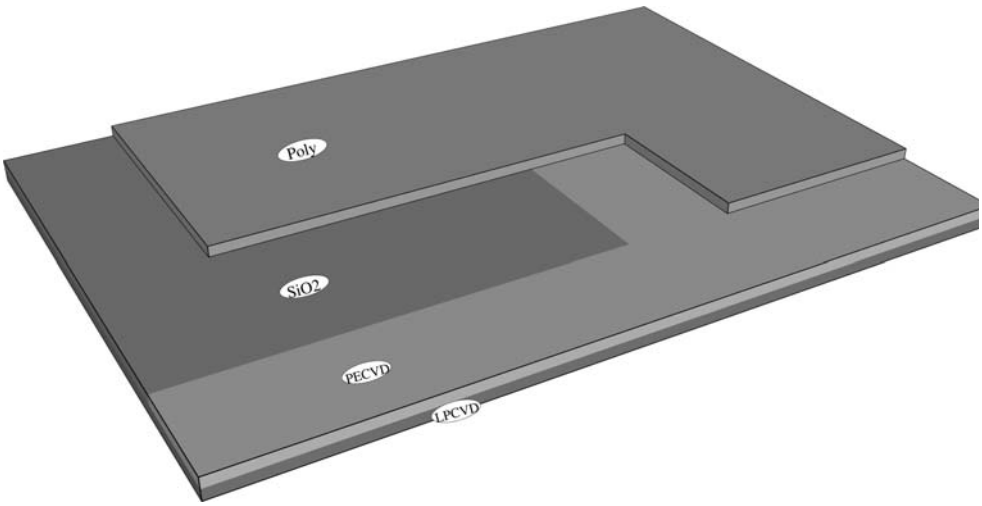

Fig. 7 Initial cantilever structure. The SiO_2 is etched nearly 100 times faster than the PECVD segment. The LPCVD segment is nearly not attacked

each grid point stores the distance to the etch front, i.e., a signed distance, a negative sign in direction of the remaining material, positive in the etched-away atmosphere. For the subsequent mechanical stress simulation which cannot be performed on the diffuse interface representation, the remaining material has to be converted to a volume mesh with sharp interfaces. A full etching cycle with final conversion to the volume mesh is shown in the next application.

7.2 A cantilever structure

The initial geometry represents also a polysilicon layer placed on an oxide layer. The oxide has to be removed to release the polysilicon cantilever from the substrate. Additionally the oxide layer is embedded in a PECVD layer, which has an etch speed of 1/100 of oxide (refer Fig. 7).

The result after finishing the etching process is shown in Fig. 8. The oxide layer is completely removed and the cantilever is released. Although the etch speed is low in the PECVD layer, it has been completely removed from the top, because its whole surface is exposed to the etch agent. Under the polysilicon regions the underetch of the PECVD layer can be examined. In this figure an additional tungsten layer has become visible, which was hidden before by the PECVD.

8 Outlook

As shown in the last example, the etching simulation of a quite complex structure was possible. Obviously, there is always the potential of further model improvements. One important aspect should be the inclusion of effects caused by adhesive attraction of the etchant atoms to the underlying materials. This attraction dilutes the transport of the etch agent and a lowered etch speed can be observed. The etch speed depends on the wetting angle of the etch agent on the etched material.

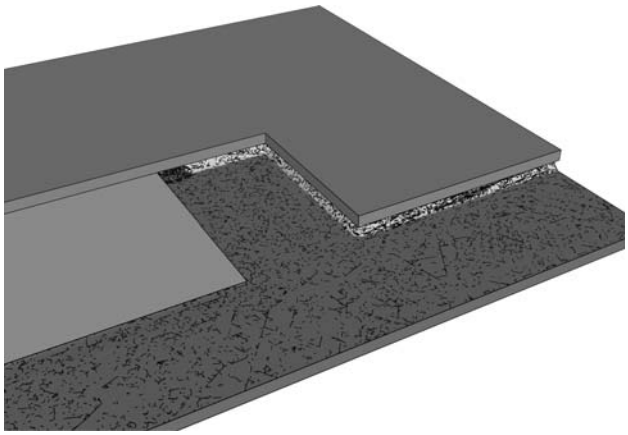

Fig. 8 Situation after reaching final time, the level-set representation is back-converted to a tetrahedral representation. SiO_2 has been removed and the Poly is free standing. Clear underetch of the PECVD layer under the Poly layer can be seen

Acknowledgments This work has been supported by the European Community *PROMENADE* project.

References

Bühler J, Steiner F-P, Baltes H (1997) Silicon dioxide sacrificial layer etching in surface micromachining. J Micromech Microeng 7(1):R1–R13

Eaton WP, Smith JH (1996) Release-etch modeling for complex surface micromachined structures. In: Pang SW, Chang S-C (eds) In: Stella WP, Shih-Chia C (eds) Proceedings SPIE, vol 2882, pp. 80-93, micromachining and microfabrication process Technology II, pp 80–93

Heitzinger C, Fugger J, Häberlen O, Selberherr S (2002) Simulation and inverse modeling of teos deposition processes using a fast level set method. In 2002 international conference on simulation of semiconductor processes and devices, pp 191–194

Liu J, Tai YC, Lee J, Pong KC, Zohar Y, Ho CM (1993) In situ monitoring and universal modeling of sacrificial PSG etching using hydrofluoric acid. In: An investigation of micro structures, sensors, actuators, machines and systems, Fort Lauderdale, Florida

Mescheder U (2004) Mikrosystemtechnik, Konzepte und Anwendungen, 2nd edn. Teubner

Monk DJ, Soane DS, Howe RT (1993) Determination of the etching kinetics for the hydrofluoric acid/silicon dioxide system. J Electrochem Soc 140(8):2339–2346

PRIME Faraday Partnership (2002) An Introduction to MEMS (Micro-Electromechanical Systems).

Rivara M, Inostroza P (1995) A discussion on mixed (longest side midpoint insertion) Delaunay techniques for the triangulation refinement problem. In 4th International Meshing Roundtable, Sandia National Labs, Albuquerque, New Mexico, pp 335–346

Sethian J (1999) Level set methods and fast marching methods. Cambridge University Press, Cambridge

Sethian J, Adalsteinsson D (1997) An overview of level set methods for etching, deposition, and lithography development. IEEE Trans Semi Manufac 10(1):167–184

Wessner W, Heitzinger C, Hössinger A, Selberherr S (2003) Error estimated driven anisotropic mesh refinement for three-dimensional diffusion simulation. In 2003 IEEE international conference on simulation of semiconductor processes and device, pp 109–112